

## Analysis of thermal effects in an end-diode-pumped, Q-switched Nd:YVO<sub>4</sub> laser

Mateusz Kaskow<sup>1</sup>, Lech. Boruc<sup>2</sup>, Lukasz Boruc<sup>2</sup>, Maciej Giemza<sup>2</sup>, Michal Piasecki<sup>1</sup>

<sup>1</sup>*Institute of Optoelectronics, Military University of Technology, gen. Sylwestra Kaliskiego 2, 00-908 Warszawa,*

<sup>2</sup>*Solaris Laser S.A, Wynalazek 4, 02-677 Warszawa.*

Received October 29, 2013; accepted November 21, 2013; published December 31, 2013

**Abstract**—We present a laboratory model of a Q-switched Nd:YVO<sub>4</sub> laser with thermal effects compensation dedicated as a laser head for marking devices. Theoretical analyses on thermal effects were performed and resonator parameters were optimized. For the 10kHz repetition rate we obtained about 0.25mJ of pulse energy corresponding to about 45kW of peak power with a slope efficiency of 14%. The  $M^2$  parameter was 1.6.

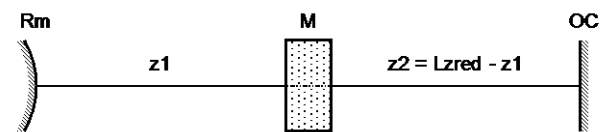


Fig. 1. Resonator scheme with inner active element with variable optical power.

Since their discovery, neodymium lasers [1] have attracted people's interest for the last 50 years. 1 $\mu$ m radiation is exploited in many areas, and a four-level laser scheme does not require a sophisticated cooling mechanism (as in ytterbium doped media) in order to achieve high energy output. Q-switched Nd doped active media have found military applications as rangefinders or laser designators. The second harmonic generation process allows to build green lasers, which are used as pump modules for Ti:S systems [2]. They offer the possibility of optical parametric generation in nonlinear crystals and shift wavelengths to mid-infrared [3]. They are also very common lasers found in cutting, welding, marking and engraving devices. Q-switched Nd doped fiber lasers [4-5] compete with bulk ones. The relation of their surface area to volume is very high, thus their heat dissipation is very good and they do not require radiators or water-cooling. However, the splices and facets are very susceptible to damage under high peak power pulses propagation. In this work we present a laboratory model of a Q-switched Nd:YVO<sub>4</sub> laser designated as a head in a marking device.

A thermo-optical lens induced by a heat load inside the gain medium is the main problem of obtaining high powers with a good beam quality. However, it can be compensated by the proper choice of resonator parameters. We elaborated a theoretical tool that enables axial analysis and optimization of a laser resonator. An active element (thermal lens) with variable optical power is located between the rear mirror ( $Rm$  – radius of curvature) and output coupler (see Fig. 1). Matrix optics (ABCD method) calculus was applied assuming linear dependence of thermo-optic power on a pump parameter (incident pump power).

The round-trip matrix is expressed by:

$$M_{RT}(L, z2, M, Rm) = T(z2) \cdot P(M) \cdot T(L - z2) \cdot P\left(\frac{-2}{Rm}\right) \cdot T(L - z2) \cdot P(M) \cdot T(z2) \quad (1)$$

where:  $M$  – variable thermo-optical power,  $T$  – translation matrix,  $P$  – refraction matrix,  $Rm$  – rear mirror radius of curvature,  $L$  – resonator length. The theoretical tool allows to analyze the influence of listed parameters on output beam parameters such as a mode radius inside the gain medium, beam divergence and estimated beam quality parameter  $M^2$ . We determined that a convex rear mirror with a radius of curvature  $Rm=250$ mm and a total resonator length of  $L=140$ mm will compensate for thermal lensing and will provide total beam divergence of less than 7mrad (which is less than the divergence angle of 1<sup>st</sup> diffraction order of an acousto-optic modulator). The mode diameter will be lower than the pump beam diameter ( $2w_p=360\mu$ m).

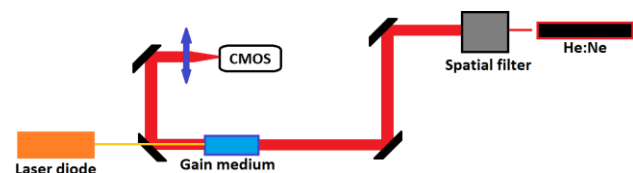


Fig. 2. Thermal effects registration setup.

Figure 2 shows the setup which was used for registration of thermal effects occurring in an active medium. He:Ne probe beam was spatially filtered and expanded. A plane wavefront passed through the thermally distorted gain

medium. An interferogram was registered on a CMOS camera.

In experiments 0.2% at. doped Nd:YVO<sub>4</sub> (3×3×10cm<sup>3</sup>) cut along a-axis was applied. It was passively cooled via forced air flow. A 30W laser diode with a central wavelength  $\lambda=808\text{nm}$  ( $T=25^\circ\text{C}$ ) was used. The pump beam was focused into an active medium. An acousto-optic modulator with total RF power  $P_{\text{RF}}=20\text{W}$  was introduced as a Q-switch. The repetition frequency range was  $f=10\div 100\text{kHz}$ . The mode radius for different thermal lenses, calculated according to the model that we elaborated, is shown in Fig. 3.

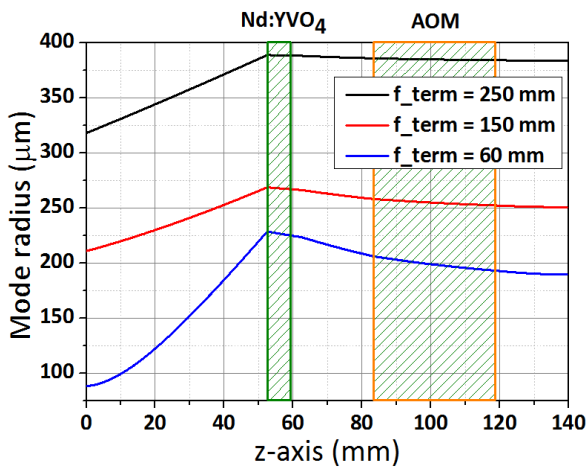


Fig. 3. Mode radius of resonator vs. z-distance for different thermal focal length values.

The longer focal length is, the narrower mode of the resonator gets. The resonator with a convex mirror compensating thermal lens is unstable. After reaching the threshold value of pump power, by inducing thermal lensing, it enters the stability region, thus narrowing the incident pump power range in which the laser operates properly.

Before setting up the resonator, we registered the interferograms of a thermally distorted wavefront (see Fig. 2). The results are shown below, in Fig. 4.

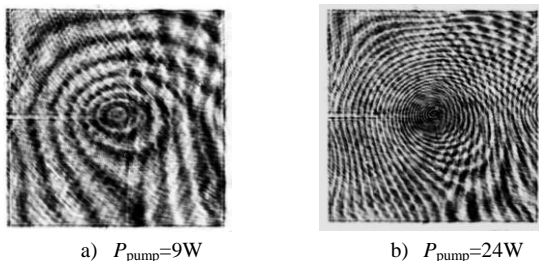


Fig. 4. Interferograms of active medium under heat load for different incident pump powers.

There is clearly visible anisotropy of heat conductivity, which value is different for the direction parallel and perpendicular to the c-axis. One can see that temperature gradients are oriented vertically and horizontally, which is indicated by proper crystal assembly and good heat removal.

The laser visualization is shown on Fig. 5.



Fig. 5. 3D model of laser setup.

In order to decrease the heat load in the active medium, the laser diode was cooled to  $T=15^\circ\text{C}$  and the central wavelength was about 806 nm. The maximum pump power, which was the thermal effects threshold, was set to  $P_{\text{pump}}=21.1\text{W}$ .

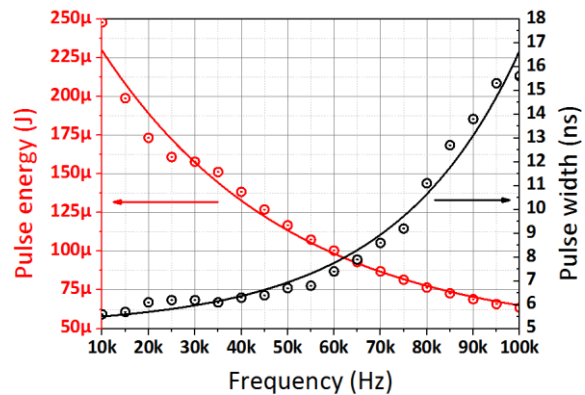


Fig. 6. Pulse energy and pulse width vs. repetition frequency for  $P_{\text{pump}}=21.1\text{W}$ .

Pulse energy with a maximum energy of about  $E = 230 \mu\text{J}$  with a pulse width below  $\tau=6\text{ns}$  for 10kHz repetition rate was obtained (Fig. 6). It corresponded to the peak power of about  $P_{\text{peak}}=45\text{kW}$ . The average output power was about  $P_{\text{avg}}=2.5\text{W}$ . The slope efficiency was  $\eta=14\%$ . For 100kHz, the obtained pulse energy was about  $E=60\mu\text{J}$ , pulse width was about  $\tau=16\text{ns}$  and peak power was below  $P_{\text{peak}}=5\text{kW}$ . The average power reached  $P_{\text{avg}}=6.5\text{W}$  and slope efficiency  $\eta=47\%$ . The total beam divergence was below  $\Theta < 3.8\text{mrad}$  in the full repetition frequency range.

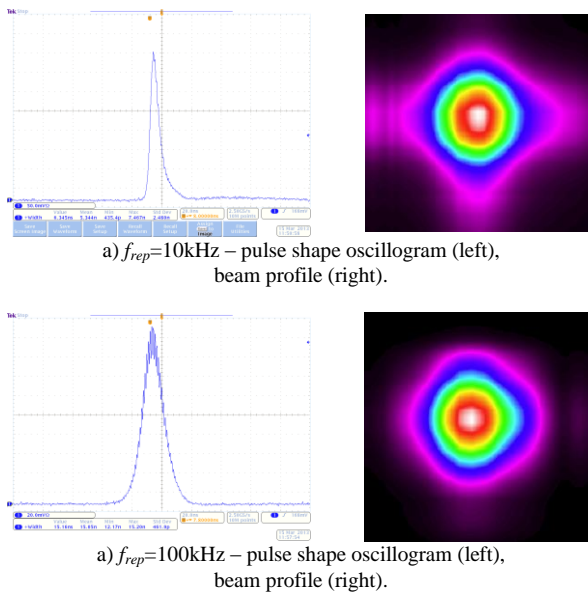


Fig. 7. Oscilloscope of pulse shape (left column) and beam profile (right column) of laser beam for 10kHz and 100kHz repetition frequency.

Figure 7 shows an oscilloscope of the pulse shape and spatial beam profile registered with a slit beam profiler. There are no thermal effects. The sidebands in Fig. 7a are caused by beam integration for lower frequencies. The pulse shape is well defined and indicates multimode generation. The beam quality parameter  $M^2$  was measured. For 10kHz repetition frequency the beam quality parameter was  $M^2=1.6$  and for 100kHz it decreased to 1.13. The output beam is near diffraction-limited (see Fig. 8).

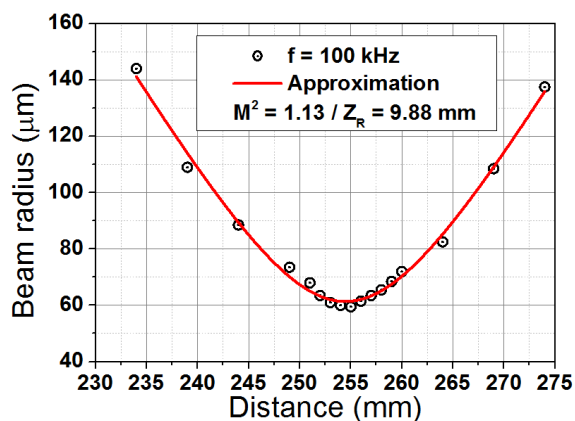


Fig. 7. Beam radius vs.  $z$ -distance from lens for  $f = 100\text{kHz}$ .

In summary, a simple, axial model of a laser resonator with an active element with variable optical power was elaborated. It enables proper choice of resonator parameters in order to obtain the required mode radius

and divergence. It allows to estimate the beam quality parameter  $M^2$ , as well.

Energetic characteristics for maximum pump power (below thermal effects threshold,  $P_{th}=22\text{W}$ ) were measured. The following results were obtained: for 10kHz:  $E=0.247\text{mJ}$ ,  $\tau=5.6\text{ns}$ ,  $P_{avg}=2.47\text{W}$ ,  $\Theta=3.75\text{mrad}$ ; for 50kHz:  $E=0.116\text{mJ}$ ,  $\tau=6.7\text{ns}$ ,  $P_{avg}=5.83\text{W}$ ,  $\Theta=3.6\text{mrad}$ ; and for 100kHz:  $E=0.063\text{mJ}$ ,  $\tau=15.6\text{ns}$ ,  $P_{avg}=6.35\text{W}$ ,  $\Theta=3.5\text{mrad}$ .

This research has been supported by the Polish National Centre for Research and Development under Project No. INNOTECH-K1/IN1/4/156909/NCBR/12.

## References

- [1] J.E. Geusic, H.M. Marcos, L.G. Van Uitert, Appl. Phys. Lett. **4** (10), (1964).
- [2] L. Gorajek, L. Galecki, Phot. Lett. Poland **1**(3), 136 (2009).
- [3] W. Zendzian, J.K. Jabczynski, P. Wachulak, J. Kwiatkowski, Appl. Phys. B **80**, 329 (2005).
- [4] J. Swiderski, A. Zajac, P. Konieczny, M. Skorczakowski, Opt. Expr. **12**, 3554 (2004).
- [5] J. Swiderski, A. Zajac, P. Konieczny, M. Skorczakowski, Opto-Electr. Rev. **13**(3), 29 (2005).